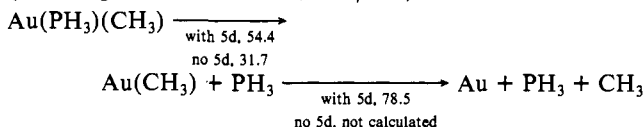


**Table XIII.** Decomposition of the Total Bond Energy between AuCH<sub>3</sub> and PH<sub>3</sub> (kcal/mol)

term	Au 5d in valence	Au 5d in core
$\Delta E(\text{steric})$	+10.3	+10.3
$\Delta E(a_1)$	-29.7	-20.8
$\Delta E(e)$	-12.2	-3.7
total nonrelativistic	-31.6	-14.2
relativistic correction	-28.5	-23.2
relaxation of PH <sub>3</sub>	+5.7	+5.7
total	-54.4	-31.7

be 105° in our calculations. The effect of changing the bond angle of PH<sub>3</sub> from its experimental value of 93 degrees to 105 degrees is quite dramatic on the lowest computed ionization energy: 10.23 vs. 9.41 eV, respectively. Since the experimental IE of PMe<sub>3</sub> is 8.62 eV,<sup>11</sup> the perturbed PH<sub>3</sub> ligand already is able to mimic this donor orbital aspect of the PMe<sub>3</sub> ligand.

Our binding energy results indicate the following energetics (including relativistic effects, kcal/mol):



The breakdown of the energy terms with respect to the Au(CH<sub>3</sub>)

and PH<sub>3</sub> fragments is presented in Table XIII both with and without 5d orbitals in the valence set for the first step of this reaction. We were particularly interested in determining whether there was more d orbital involvement in the gold compound than in the mercury compounds discussed earlier. Inspection of the results given in Table XIII shows that such is indeed the case. About 40% of the Au-PH<sub>3</sub> binding is lost upon removal of the Au 5d orbitals from the basis set. This is as expected, since the Au 5d orbitals are much more energetically available than the Hg 5d orbitals. Our calculations indicate that the Au 5d orbital involvement is large in contrast to the conclusions of Bancroft et al.,<sup>11</sup> based upon their interpretation of the UP spectra. The increased involvement of Au 5d over Hg 5d is in line with the lesser Mulliken population of the Au 5d<sub>σ</sub> orbital compared to the Hg 5d<sub>σ</sub> orbital (Tables II, V, and VIII).

**Acknowledgment.** This work was supported in part by financial aid from the Netherlands Organization for the Advancement of Pure Research (ZWO). R.D.K. also acknowledges the grant support of the Netherlands America Commission for Educational Exchange and of Calvin College for a Calvin Research Fellowship. We gratefully acknowledge helpful discussions with Dr. J. G. Snijders.

**Registry No.** Hg(CH<sub>3</sub>)<sub>2</sub>, 593-74-8; Hg(CN)<sub>2</sub>, 592-04-1; Hg(CH<sub>3</sub>)(CN), 2597-97-9; Hg(CCCCH<sub>3</sub>)<sub>2</sub>, 64705-15-3; Au(PMe<sub>3</sub>)(CH<sub>3</sub>), 32407-79-7.

## Protonation Equilibria and Charge Transport in Electroactive Tetracyanoquinodimethane Polymer Films

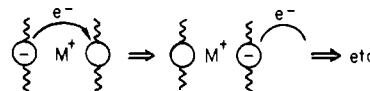
György Inzelt,<sup>1</sup> James Q. Chambers,\* James F. Kinstle, and Roger W. Day

Contribution from the Department of Chemistry, University of Tennessee, Knoxville, Tennessee 37996-1600. Received August 1, 1983

**Abstract:** The electrochemical behavior and electron spin resonance response of thin films of tetracyanoquinodimethane polyester in contact with aqueous buffers have been studied. The results indicate that the coupling of electron- and proton-transfer steps in the classical 3 × 3 square scheme, which describes quinone electrochemistry, can significantly influence the charge-transport rate through the film, limiting the electroactivity to a fraction of the available electron-transfer sites and decreasing the effective diffusion coefficient for charge transport through the polymer film by 100-fold for specific conditions. The acid-base chemistry of the reduced acceptor sites in the film matrix accounts for the pH dependence of the voltammetric waves, the film passivation in acidic solutions, and the film dissolution at negative potentials in simple salt electrolytes. The acid dissociation constants of the reduced acceptor sites in the polymer matrix are estimated from the pH dependence of the E<sub>1/2</sub> values—for TCNQH<sub>2</sub> pK<sub>a</sub> values of 6.9 ± 0.1 and 10 are obtained in aqueous phosphate buffers.

In the few years since the initial reports on the modification of electrodes with electroactive polymers,<sup>2-4</sup> the variety of systems studied, and the concomitant theories and applications, have mushroomed and are continuing to increase.<sup>5</sup> Intense interest has focused on electrocatalysis using polymer modified electrodes<sup>6</sup> and on electronically conducting polymer films based on poly(pyrrole),<sup>7</sup> poly(acetylene),<sup>8</sup> and related materials,<sup>9</sup> although other

Scheme I



significant applications have appeared on the horizon. Included among the latter are electrochromic devices,<sup>10</sup> electrochemical desalination electrolysis,<sup>11</sup> neurotransmitter stimulating electrodes,<sup>12</sup> coatings for the stabilization of semiconductor photo-

(1) Department of Physical Chemistry and Radiology, L. Eötvös University, Budapest, Hungary.

(2) Merz, A.; Bard, A. J. *J. Am. Chem. Soc.* **1978**, *100*, 3222.

(3) Van De Mark, M. R.; Miller, L. L. *J. Am. Chem. Soc.* **1978**, *100*, 3223.

(4) Kaufman, F. B.; Engler, E. M. *J. Am. Chem. Soc.* **1979**, *101*, 547.

(5) Albery, W. J.; Hillman, A. R. *R. Soc. Chem., Annu. Reports C* **1981**, *78*, 377.

(6) Anson, F. C.; Ohsaka, T.; Saveant, J.-M. *J. Am. Chem. Soc.* **1983**, *105*, 4883.

(7) Kanazawa, K. K.; Diaz, A. F.; Geiss, R. H.; Gill, W. D.; Kwak, J. F.; Logan, J. A.; Rabolt, J. F.; Street, G. B. *J. Chem. Soc., Chem. Commun.* **1979**, 854.

(8) MacInnes, D., Jr.; Druy, M. A.; Nigrey, P. J.; Nairns, D. P.; MacDiarmid, A. G.; Heeger, A. J. *J. Chem. Soc., Chem. Commun.* **1981**, 317.

(9) (a) Chance, R. R.; Shacklette, G. G.; Miller, G. G.; Ivory, D. M.; Sowa, J. M.; Elsenbaumer, R. L.; Baughman, R. H. *J. Chem. Soc. Chem. Commun.* **1980**, 348. (b) Rabolt, J. F.; Clarke, T. C.; Kanazawa, K. K.; Reynolds, J. R.; Street, G. B. *Ibid.* **1980**, 347. (c) Waltman, R. J.; Bargon, J.; Diaz, A. F. *J. Phys. Chem.* **1983**, *87*, 1459. (d) Kaneto, K.; Kohno, Y.; Yoshino, K.; Inuishi, Y. *J. Chem. Soc., Chem. Commun.* **1983**, 382. (e) Shacklette, L. W.; Elsenbaumer, R. L.; Chance, R. R.; Sowa, J. M.; Ivory, D. M.; Miller, G. G.; Baughman, R. H. *Ibid.* **1982**, 361.

(10) Desbene-Monvernay, A.; Lacaze, P. C.; Dubois, J. E.; Desbene, P. L. *J. Electroanal. Chem. Interfacial Electrochem.* **1983**, *152*, 87.

(11) Factor, A.; Rouse, T. O. *J. Electrochem. Soc.* **1980**, *127*, 1313.

voltaic electrodes,<sup>13</sup> ion gating devices,<sup>14</sup> and bilayer electrodes having possible application in microelectronics.<sup>15</sup>

A central theme in this area has been the mechanism of charge transport through electroactive polymer films. For most applications envisioned, facile charge transport throughout the film electrode material is desired such that the films are fully electroactive and have rapid response times. For switching devices, such as the ion gate and charge trapping, bilayer electrodes of Murray and co-workers,<sup>15,16</sup> rapid transitions between highly insulating and conducting states are desired. The rate of charge transport, however, as characterized by an effective diffusion coefficient for charge transport,  $D_{ct}$ , can vary over several orders of magnitude ( $10^{-7}$  to  $10^{-14}$  cm<sup>2</sup> s<sup>-1</sup>) for electroactive polymer films.<sup>16</sup> These values can lead to extremely long times for oxidation or reduction of thin films; e.g., for films of 100-nm thickness these  $D_{ct}$  values correspond to times from 3 ms to 7.5 h for full (99.9%) electrode charging.<sup>17</sup>

Factors governing the magnitude of  $D_{ct}$  for various electroactive polymers are not well understood. As recognized by the early workers in this area,<sup>4</sup> for fixed-site electroactive polymers in the absence of mediators, an electron-hopping charge-transport mechanism is operative. Charge propagates through these films by electron-exchange reactions between adjacent sites in the polymer matrix as shown in Scheme I for an electron-acceptor polymer. As pointed out by Buttry and Anson<sup>18</sup> and others,<sup>19</sup> in this situation the Dahms-Ruff electron-hopping charge-transport mechanism,<sup>20-22</sup> which was originally developed for solutions, can be applied. Since the electron-transfer sites are fixed, the effective charge-transport diffusion coefficient is given by the expression

$$D_{ct} = (\text{constant})k_{ex}\delta^2C \quad (1)$$

where  $k_{ex}$  is the second-order exchange rate constant,  $\delta$  is the distance between the sites, and  $C$  is the concentration of exchange sites. Rapid charge transport is therefore favored by proper alignment and high density of the exchange sites in the polymer matrix. The concentration dependence of  $D_{ct}$  has been nicely documented for the transition-metal bipyridyl redox polymer films of Murray and co-workers.<sup>23</sup>

The electron-hopping process pictured in Scheme I will necessarily require ion migration in order to maintain electrical neutrality in the polymer film phase and may involve motions of the polymer backbone. The latter could open channels for counterions migration or align exchange sites for the electron hop. In order to probe the role of the counterion several groups have studied electrolyte effects on the charge-transport process in polymer film electrodes. The results are complicated by the fact that charging a polymer film usually involves large changes of film ionic conductivity and an accompanying variable uncom-

pensated resistance.<sup>24,25</sup> Thus ion association effects are often obscured by experimental artifacts and are difficult to distinguish from changes in the uncompensated resistance. However, ion association effects have been reported for poly(vinylferrocene),<sup>25,26</sup> poly(tetrathiafulvalene),<sup>16,24,27</sup> and poly(tetracyanoquinodimethane) electrodes.<sup>28</sup> Other film properties may be influenced by the nature of the counterion. For example, Diaz et al. have recently observed that the tensile strength of oxidized poly(pyrrole) films is increased when organic counterions such as tosylate are employed in the electropolymerization process.<sup>29</sup>

We report here on the effect of pH on the tetracyanoquinodimethane (TCNQ) polymer film electrochemistry. Previously, these films have been studied in contact with aqueous solutions of simple unbuffered electrolytes, e.g., MX and MX<sub>2</sub>, where M = Li<sup>+</sup>, Na<sup>+</sup>, Rb<sup>+</sup>, Ca<sup>2+</sup>, and NEt<sub>4</sub><sup>+</sup> and X = Cl<sup>-</sup> and ClO<sub>4</sub><sup>-</sup>.<sup>28,30,31</sup> In contact with these electrolytes, the acceptor sites in the low molecular weight TCNQ polyesters are fully electroactive and dimerize extensively in the 1- oxidation state.<sup>31</sup> (While the 2TCNQ<sup>-</sup> ⇌ TCNQ<sub>2</sub><sup>2-</sup> dimerization equilibrium is fast on the slow sweep rate cyclic voltammetric time scale, formation of TCNQ<sub>2</sub><sup>-</sup>, where an unpaired electron is associated with two TCNQ acceptor units, presumably on different polymer chains, is much slower and accounts for the unusual shape of the voltammograms.) Electrolyte effects were observed for these films with Nernstian response found for the peak potentials of the first couple for M = Li<sup>+</sup>, Na<sup>+</sup>, and Ca<sup>2+</sup>.<sup>28</sup>

A second reduction wave with peak currents approximately equal to those of the first wave is also observed in the cyclic voltammograms for the TCNQ modified electrodes in these electrolytes. This wave is assigned to formation of the TCNQ<sub>2</sub><sup>2-</sup> dianion. In the presence of 1-1 electrolytes the film electroactivity is lost when the potential is cycled through this wave. The reason for this behavior is not fully understood, but it may be due to hydrolysis of the ester links and dissolution of the polymer film under the basic conditions generated by the TCNQ<sub>2</sub><sup>2-</sup> sites. In the presence of calcium salts, however, the second wave is reproducible and the film can be cycled continuously through the 0/-2- oxidation states without decreasing the film electroactivity.<sup>28</sup>

In the presence of appropriate buffer components the TCNQ film electroactivity undergoes dramatic changes. The charge-transport process for the second wave is markedly dependent on the solution pH. This is a result of the coupling of protonation and electron-transfer steps in the classical 3 × 3 square scheme that describes quinone electrochemistry in aqueous or nonaqueous protic solutions.<sup>32</sup> Experiments documenting these effects, which have important implications for the design of polymer-modified electrodes and the understanding of charge transport in electroactive polymer films, are described below.

## Experimental Section

**Chemicals.** The TCNQ polymer used in this study was synthesized from the 2,5-bis(2-hydroxyethoxy)-7,7,8,8-tetracyanoquinodimethane monomer of Hertler<sup>33</sup> and has been described previously.<sup>30,34</sup> Essentially identical results have now been obtained by using material from four independent preparations of the polyester with adipoyl chloride as the

(12) (a) Lau, A. N. K.; Miller, L. L. *J. Am. Chem. Soc.*, **1983**, *105*, 5271. (b) Lau, A. N. K.; Miller, L. L.; Zinger, B. *Ibid.* **1983**, *105*, 5178.

(13) (a) Fan, F. F.; Wheeler, B. L.; Bard, A. J.; Noufi, R. N. *J. Electrochem. Soc.* **1981**, *128*, 2042. (b) Noufi, R.; Tench, D.; Warren, L. F. *J. Electrochem. Soc.* **1981**, *128*, 2596; **1980**, *127*, 2310. (c) Skotheim, T.; Petersson, L.-G.; Inganäs, O.; Lundström, I. *Ibid.* **1982**, *129*, 1737. (d) Frank, A. J.; Honda, K. *J. Phys. Chem.* **1982**, *86*, 1933. (e) Skotheim, T.; Lundström, I.; Prejza, J. *J. Electrochem. Soc.* **1981**, *128*, 1042.

(14) Burgmayer, P.; Murray, R. W. *J. Am. Chem. Soc.* **1982**, *104*, 6139.

(15) Denisevich, P.; Willman, K. W.; Murray, R. W. *J. Am. Chem. Soc.* **1981**, *103*, 4727.

(16) Schroeder, A. H.; Kaufman, F. B. *J. Electroanal. Chem. Interfacial Electrochem.* **1980**, *113*, 209.

(17) Chambers, J. Q. *J. Electroanal. Chem. Interfacial Electrochem.* **1981**, *130*, 381.

(18) (a) Buttry, D. A.; Anson, F. C. *J. Electroanal. Chem. Interfacial Electrochem.* **1981**, *130*, 333. (b) Buttry, D. A.; Anson, F. C. *J. Am. Chem. Soc.* **1983**, *105*, 685.

(19) White, H. S.; Leddy, J.; Bard, A. J. *J. Am. Chem. Soc.* **1982**, *104*, 4811.

(20) Dahms, H. *J. Phys. Chem.* **1968**, *72*, 362.

(21) (a) Ruff, I. *Electrochim. Acta* **1970**, *15*, 1059. (b) Ruff, I.; Friedrich, V. *J. Phys. Chem.* **1971**, *75*, 3297. (c) Ruff, I.; Friedrich, V.; Demeter, K.; Csillag, K. *Ibid.* **1971**, *75*, 3303. (d) Ruff, I.; Friedrich, V.; Csillag, K. *Ibid.* **1972**, *76*, 162. (e) Ruff, I.; Friedrich, V. *Ibid.* **1972**, *76*, 2954, 2957.

(22) Lengyel, S. *Magy. Kem. Foly.* **1974**, *80*, 187.

(23) (a) Facci, J. S.; Schmehl, R. H.; Murray, R. W. *J. Am. Chem. Soc.* **1982**, *104*, 4959. (b) Schmehl, R. H.; Murray, R. W. *J. Electroanal. Chem. Interfacial Electrochem.* **1983**, *152*, 97.

(24) Kaufman, F. B.; Schroeder, A. H.; Engler, E. M.; Kramer, S. R.; Chambers, J. Q. *J. Am. Chem. Soc.* **1980**, *102*, 483.

(25) Daum, P.; Murray, R. W. *J. Phys. Chem.* **1981**, *85*, 389.

(26) Pearce, P. J.; Bard, A. J. *J. Electroanal. Chem. Interfacial Electrochem.* **1980**, *112*, 97; **1980**, *114*, 89.

(27) Chambers, J. Q.; Kaufman, F. B.; Nichols, K. H. *J. Electroanal. Chem. Interfacial Electrochem.* **1982**, *142*, 277.

(28) Inzelt, G.; Day, R. W.; Kinstle, J. F.; Chambers, J. Q. *J. Electroanal. Chem. Interfacial Electrochem.* **1984**, *161*, 147.

(29) Diaz, A. F.; Hall, B. *IBM J. Res. Dev.* **1983**, *27*, 342.

(30) Day, R. W.; Inzelt, G.; Kinstle, J. F.; Chambers, J. Q. *J. Am. Chem. Soc.* **1982**, *104*, 6804.

(31) Inzelt, G.; Day, R. W.; Kinstle, J. F.; Chambers, J. Q. *J. Phys. Chem.* **1983**, *87*, 4592.

(32) Chambers, J. Q. In "The Chemistry of the Quinoid Compounds"; Patai, S., Ed.; John Wiley: London, 1974; Chapter 14.

(33) Hertler, W. R. *J. Org. Chem.* **1976**, *41*, 1412.

(34) Day, R. W. Ph.D. Thesis, University of Tennessee, Knoxville, 1984.

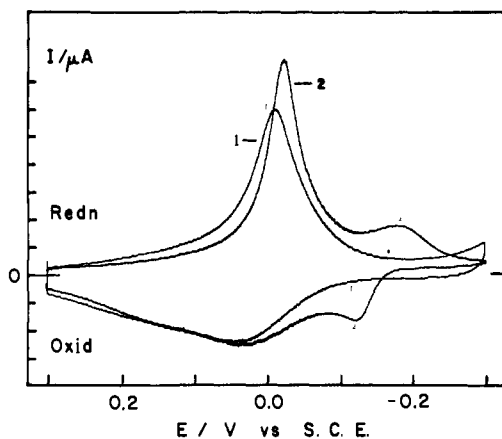


**Figure 1.** Cyclic voltammograms of a 30-nm-thick TCNQ film electrode in contact with a (1) 0.5 mol dm<sup>-3</sup> NaClO<sub>4</sub> and (2) 0.25 mol dm<sup>-3</sup> NaClO<sub>4</sub>, 0.25 mol dm<sup>-3</sup> phosphate pH 7 solution: sweep rate, 10 mV s<sup>-1</sup>; current axis, 2 μA per division; electrode area, 0.196 cm<sup>2</sup>.

comonomer. Analytical grade NaCl, NaClO<sub>4</sub>, NaOH, Na<sub>3</sub>PO<sub>4</sub>, Na<sub>2</sub>HPO<sub>4</sub>, NaC<sub>2</sub>H<sub>3</sub>O<sub>2</sub>, HC<sub>2</sub>H<sub>3</sub>O<sub>2</sub> (all Fisher Scientific), and NaH<sub>2</sub>PO<sub>4</sub> (Merck) were used. Recrystallized phosphate salts were used for preparation of the buffer solutions.

The polymer film electrode preparation procedures have been described previously.<sup>30</sup> For most of the studies, the films were coated on metallized quartz disks that served as windows in an all-Teflon cell. The coated disks were usually baked for 2–3 min at 130 °C; this procedure improved the film stability upon repeated electrochemical cycling. Simultaneous spectrophotometry and cyclic voltammetry was carried out with the cell placed in the sample compartment of a Carry 171 spectrophotometer using a potentiostat and sweep generator of conventional design. The simultaneous electrochemical electron spin resonance (SEESR) experiments<sup>35</sup> were performed on polymer films that had been dip-coated onto platinum grid substrates. The solutions were thoroughly purged with argon or nitrogen before recording the voltammograms. The presence of trace amounts of oxygen, however, did not noticeably affect the results.

## Results and Discussion

The TCNQ polymer film electrodes in neutral unbuffered solutions exhibit a break-in phenomenon typical of electroactive polymers that are coated onto substrates in the neutral form. Thus for films of "ordinary" thickness (ca. 100 nm) several potential cycles are required for the electrodes to attain full electroactivity. Once the films are fully broken-in, however, the TCNQ films may be repeatedly and reproducibly cycled through the TCNQ<sup>0/-</sup> redox process. These effects have been documented in previous publications from this laboratory.<sup>28,31</sup> Most of the results reported below were obtained on films that had been electrochemically cycled, in separate experiments, in an appropriate electrolyte.

The break-in process is believed to be related to the uptake of electrolyte and solvent driven by the redox process. There is tentative evidence that for these TCNQ films, incorporation of the electrolyte proceeds by layers as the films are cycled. For thick films this may require many cycles (>10) in a cyclic voltammetric experiment. Incorporation of the solvent/electrolyte in this fashion essentially decreases the film resistance rendering it electroactive.

**pH Effects on Cyclic Voltammetry.** The effect of buffer species on the film electrochemistry is shown in Figure 1. Cyclic voltammogram 1 in this figure was obtained on a thin (ca. 30-nm thick) TCNQ film electrode in contact with a neutral 0.5 M NaClO<sub>4</sub> electrolyte after several cycles of the "break-in" process. The usual voltammetric behavior is exhibited for the TCNQ<sup>0/-</sup> wave; a mixture of TCNQ<sup>•-</sup> and TCNQ<sub>2</sub><sup>-</sup> reduced acceptor sites is produced in the wave at 0.0 V vs. SCE. When the potential sweep is extended past the -0.3-V limit, a second wave due to the TCNQ<sup>-/2-</sup> couple of approximately equal height as the first is seen at ca. -0.35 V. The rising current at the switching potential in the voltammogram of Figure 1 is on the foot of this second wave.

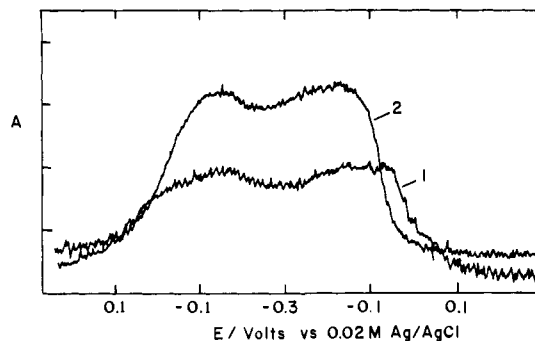


**Figure 2.** Variation of film absorbance with electrode potential at  $\lambda_1 = 830$  nm and  $\lambda_2 = 655$  nm with 0.1 absorbance unit per division. The electrode is in contact with a pH 7, 0.5 mol dm<sup>-3</sup> phosphate buffer with a sweep rate of 5 mV s<sup>-1</sup>. The potential sweep begins at the right; one complete cycle, 0.3 to -0.3 to 0.3 V, is shown.

Voltammogram 2 in Figure 1 was obtained when the 0.5 M NaClO<sub>4</sub> electrolyte was replaced with a phosphate buffer solution, pH 7, of approximately equal sodium ion concentration as the electrolyte used for voltammogram 1. The TCNQ<sup>-/2-</sup> wave, the second one-electron reversible wave, is "replaced" with a much diminished pH-dependent reversible couple (wave X) that appears at more positive potentials than the TCNQ<sup>-/2-</sup> wave in the NaClO<sub>4</sub> electrolyte. When the potential sweep is extended to  $E < -0.3$  V, the only effect is to increase somewhat the anodic peak height of wave X—the original TCNQ<sup>-/2-</sup> wave is not seen. The film electrode can be cycled repeatedly through the TCNQ<sup>0/-</sup> wave and wave X in the phosphate buffer without degradation of the response. These effects are not specific for phosphate buffers. Similar response in the pH range 5–7 was obtained for acetate buffer solutions.

When the buffer solution is now replaced with the original NaClO<sub>4</sub> solution, however, wave X disappears after the first one or two cycles and the original voltammetric response is restored in a "reverse break-in" process. This reversibility is a significant aspect of the electrolyte effects reported in this paper. Dramatic changes in the electrochemical behavior are observed for these films in the presence of appropriate electrolyte buffer components, but as revealed by the film absorption curves and the voltammograms, the films have not undergone irreversible chemical changes. Returning the films to a simple salt electrolyte restores the initial electroactivity. The implication is that the electrolyte effects are primarily operative on the charge-transport mechanism, i.e., the electron-hopping and/or ion-migration steps.

Absorbance changes as a function of potential due to the monomer radical anion species (TCNQ<sup>•-</sup>;  $\lambda = 830$  nm) and the dimer dianion species (TCNQ<sub>2</sub><sup>-</sup>;  $\lambda = 635$  nm) are shown in Figure 2. In the region of wave X the absorbance of both the radical anion and the dianion decrease to approximately the same extent consistent with the equilibrium nature of the dimerization process. Significantly, the absorbance measurements reveal that only a small fraction of the TCNQ sites in the -1 oxidation state is further reduced in the process responsible for wave X.

Wave X has more diffusional character than the TCNQ<sup>0/-</sup> wave in these voltammograms. Evidence of this is shown in Figure 3 in which the effect of variation of sweep rate is documented. These voltammograms were recorded on the same TCNQ film at sweep rates of 2, 5, 10, and 20 mV/s. As the sweep rate increases, the peak current for wave X becomes less prominent relative to the TCNQ<sup>0/-</sup> wave. The peak current is found to be proportional to  $v^{0.85}$  for the first wave and  $v^{0.51}$  for wave X. These values are to be compared to  $v^{1.0}$  and  $v^{0.5}$ , the theoretical sweep rate dependence for thin-layer "surface waves" and diffusion control, respectively. Thus for the film thickness and sweep rate range of the experiment depicted in Figure 3, close to thin-layer electrochemistry is observed for the first wave, while diffusional character is seen for wave X.

In more acidic solutions, pH < ca. 5, a more dramatic change takes place in the TCNQ film voltammetry. On the initial negative going sweep in the region of the TCNQ<sup>0/-</sup> wave, an irreversible

(35) Bard, A. J.; Faulkner, L. R. "Electrochemical Methods", John Wiley & Sons: New York, 1980; pp 614–621.

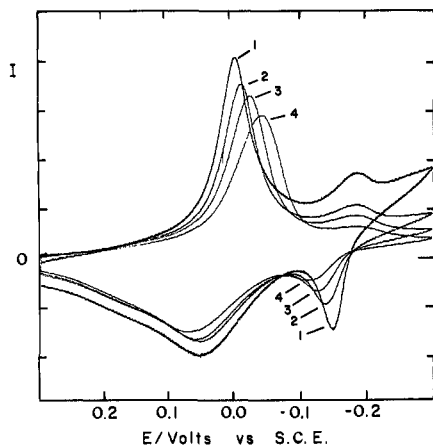


**Figure 3.** Cyclic voltammograms of a TCNQ film electrode in contact with a pH 7, 0.5 mol dm<sup>-3</sup> phosphate buffer: current axis/sweep rate (1) 20 μA/div, 2 mV s<sup>-1</sup>; (2) 50 μA/div, 5 mV s<sup>-1</sup>; (3) 100 μA/div, 10 mV s<sup>-1</sup>; and (4) 200 μA/div, 20 mV s<sup>-1</sup>.

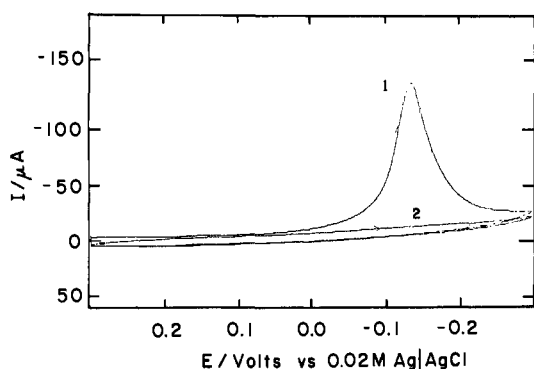


**Figure 4.** Cyclic voltammogram of a TCNQ film electrode in contact with a pH 3, 0.5 mol dm<sup>-3</sup> phosphate buffer: sweep rate, 5 mV s<sup>-1</sup>. (1) first cycle, (2) second cycle.

reduction wave is observed and the film passivates in the 0.3 to -0.3 V potential region. This behavior is shown in Figure 4 for a relatively thin TCNQ film in contact with a pH 3 solution.

The first sweep in this voltammogram displays a somewhat diminished peak current at -0.14 V. Subsequent cycles between +0.3 and -0.3 V do not show any significant faradaic current. Since the films passivate in acidic solutions, these experiments had to be carried out on films that had not been repeatedly cycled in the pH 3 electrolyte solution. This accounts for two features of the voltammogram of Figure 4 which are revealed by close examination of the data. First the peak potential is not representative of the values found for TCNQ films that have been broken-in by the cycling process in neutral solution. The peak potential is somewhat more negative than is typical for the TCNQ<sup>0/-</sup> wave for a cycled film electrode, and the peak height and total cathodic charge are significantly less than expected for full electroactivity of the polymer films. The passivation phenomenon has shut the film electrochemistry down limiting the electroactivity to a fraction of the electroactive sites.

Although the TCNQ films have become electroinactive in this potential region, they have not undergone an irreversible chemical transformation or dissolution process. They remain intact on the electrode substrate and can be restored to their original electroactivity. A clear demonstration of this result is given by the spectroelectrochemical experiment shown in Figure 5. Absorption spectrum 1 in this Figure was obtained on a TCNQ film in the neutral or oxidized form in contact with pH 3 phosphate buffer. The characteristic double-peaked band of neutral TCNQ is evident in this spectrum. Spectrum 2, obtained after the film potential had been taken through two complete potential cycles, clearly shows that a large fraction (≈0.5) of the TCNQ sites remains intact. When the film electrode was potentiostated at -0.2 V (spectrum 3), the spectrum did not change significantly. This

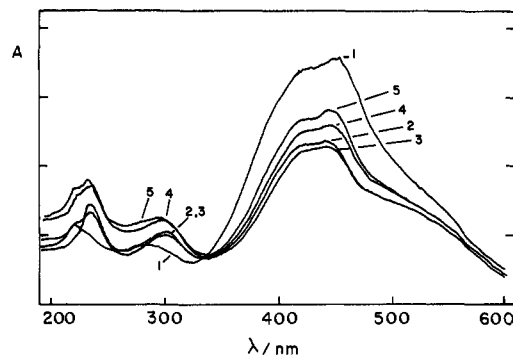
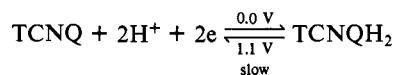


**Figure 5.** Visible-ultraviolet absorption spectra of a TCNQ film electrode in contact with a pH 3, 0.5 mol dm<sup>-3</sup> phosphate buffer; 0.2 absorbance unit per division: (1) open circuit after potential cycling at pH 7, (2) +0.3 V vs. 0.02 M Ag/AgCl after two cycles at pH 3 (see Figure 4), (3) -0.2 V, (4) +1.13 V, and (5) 1.13 V after 10 min.

is consistent with the passivation behavior displayed in Figure 3. No significant increases in the region of 600–900 nm were observed that could be assigned to radical anion or dimer dianion sites. Small absorbance changes were observed in the region of 310 and 235 nm that could be due to protonated reduced quinone sites (see below).<sup>36</sup> This region was difficult to study owing to the overlap of the intense TCNQ bands with the much weaker bands of the suspected hydroquinone-type products.

The electroactivity of films passivated at -0.3 V in acidic solutions could be restored in two ways. When the electrolyte was replaced with 0.5 M MClO<sub>4</sub> (M = Na<sup>+</sup> or Li<sup>+</sup>) or phosphate buffer of pH 6–8, the full electroactivity, as judged by the cyclic voltammetric and spectroelectrochemical behavior, was restored after several potential cycles between 0.3 and -0.3 V. Also electrochemical oxidation of the film at potentials more positive than 0.3 V partially restored the TCNQ film electroactivity. Oxidation at 1.1 V vs. SCE slowly regenerates the quinone bands as shown by curves 4 and 5 in the spectroelectrochemical experiment of Figure 5. No anodic peak currents are observed in the film voltammetry under these conditions. Indeed, a 10-min electrolysis was required to generate curve 5 of Figure 5. After this anodic electrolysis, a negative-going potential sweep revealed a cathodic wave, assigned to the reduction of regenerated TCNQ sites, and then passivation again.

*These results indicate that in acidic media the electron-transfer sites in these polymer films are reduced to the hydroquinone analogue, TCNQH<sub>2</sub>, and that in this form, the polymer does not support a facile charge-transport process.*



We suggest that formation of a nonconducting, fully reduced, protonated TCNQH<sub>2</sub> layer insulates the TCNQ sites in the bulk of the film. It seems likely that this insulating layer is formed at the polymer/solution interface, although in principle it could be located in any region of the film. The thickness of such a layer can be estimated at 20–50 nm from the charge under the peak voltammograms. This behavior is reminiscent of the hydroquinone polymer films of Miller and co-workers that display electroactivity limited to a few monolayers at most.<sup>37</sup>

Support for this interpretation of the voltammetric behavior comes from a careful examination of the behavior of wave X in the region of pH 5–8. Figure 6 shows the cyclic voltammetry of a single TCNQ film in a series of buffer solutions between pH 5.8 and 8. At pH 5.8 and 6.0 where the voltammograms are considerably drawn-out (see curves 1 and 2 in Figure 6) the film displays behavior intermediate between the pH 7 behavior of Figure 1 and the pH 3 behavior of Figure 4. As the pH is increased there is a sharp transition to full electroactivity for the

(36) Yamagishi, A.; Sakamoto, M. *Bull. Chem. Soc. Jpn.* **1974**, *47*, 2152.

(37) Fukui, M.; Kitani, A.; Degrand, C.; Miller, L. L. *J. Am. Chem. Soc.* **1982**, *104*, 28.

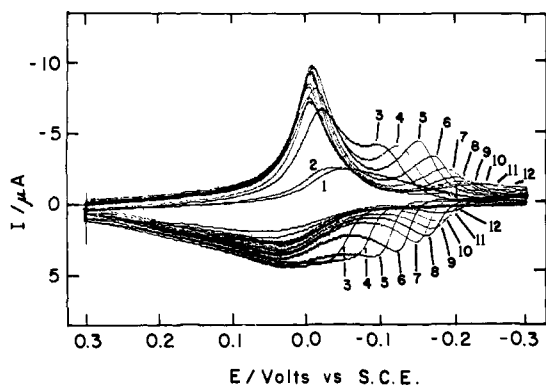


**Figure 6.** Cyclic voltammograms of a TCNQ film electrode in contact with  $0.5 \text{ mol dm}^{-3}$  phosphate buffer solutions: pH (1) 5.8, (2) 6.0, (3) 6.2, (4) 6.4, (5) 6.6, (6) 6.8, (7) 7.0, (8) 7.2, (9) 7.4, (10) 7.6, (11) 7.8, and (12) 8.0; sweep rate,  $5 \text{ mV s}^{-1}$ .

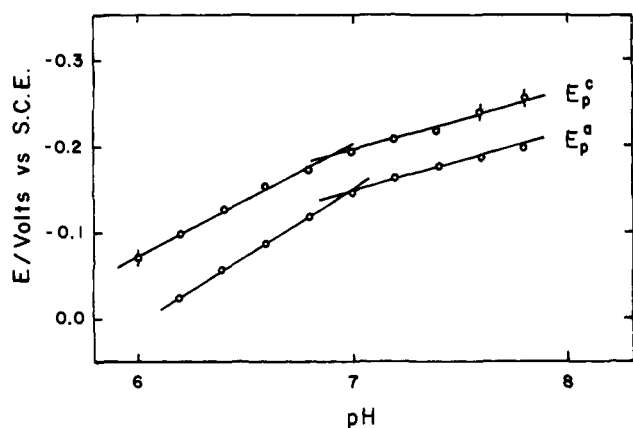


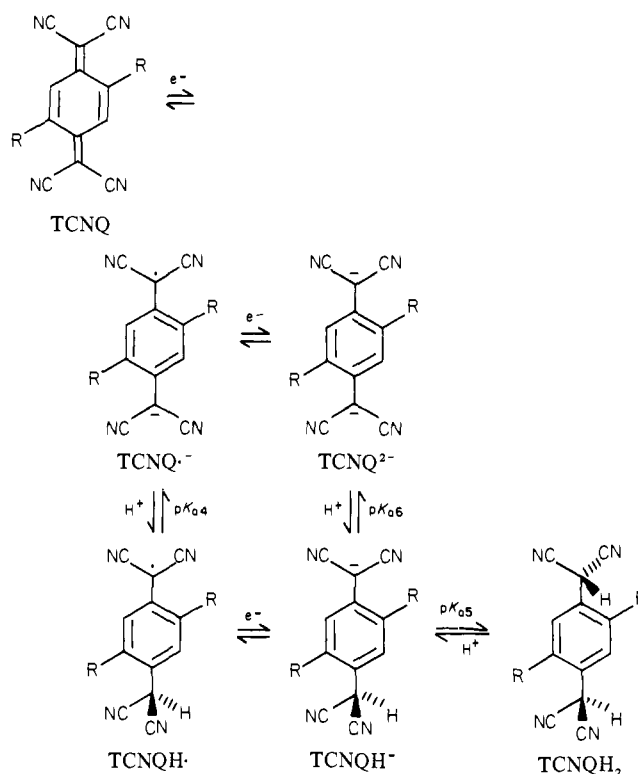
**Figure 7.** Variation with pH of  $E_{pc}$  and  $E_{pa}$  for the  $\text{TCNQ}^{0-}/\text{TCNQH}^-$  wave in a  $0.5 \text{ mol/dm}^3$  phosphate buffer; sweep rate,  $5 \text{ mV s}^{-1}$ . Data from Figure 6.

$\text{TCNQ}^{0-}$  wave and wave X becomes fully developed. In this region the  $\text{TCNQ}^{0-}$  wave is not pH dependent, while wave X shifts to more negative potentials as the pH increases. This wave is most clearly defined in the pH region 6.4 to 7.0, curves 4–7 in Figure 6.

The pH dependence of the  $E_{1/2}$  for wave X, given by  $(E_p^a + E_p^c)/2$ , strongly suggests that protonation of the reduced sites occurs to form  $\text{TCNQH}^-$  and  $\text{TCNQH}_2$  in the process responsible for wave X. The plots of peak potential for both the anodic and cathodic waves, see Figure 7, show two linear regions with slopes of 60 and 120 mV in accord with the equilibrium diagram of Laviron<sup>38</sup> for the "NN case" in the pH region where the  $e\text{H}^+$  and  $e\text{H}^+e\text{H}^+$  reaction sequences predominate. This interpretation assigns wave X to a  $\text{TCNQ}^{0-}/\text{TCNQH}^-$  or  $\text{TCNQ}^{0-}/\text{TCNQH}_2$  process and explains the absence of the  $\text{TCNQ}^{-/2-}$  wave in the presence of buffer components that can either deliver a proton to the dianion or neutralize  $\text{OH}^-$  ions formed by hydrolysis of the dianion sites. Owing to the basic character of the TCNQ anions (see below), the hydroxide ion concentration will be appreciable (up to  $10^{-2} \text{ M}$ ) in the reduced films in the absence of buffer components.

The pertinent segment of the nine-membered square scheme for TCNQ reduction is shown in Scheme II, where the notation of Laviron<sup>38</sup> has been employed. The NN case for this part of the scheme corresponds to  $\text{TCNQH}_2$  being a weaker acid than  $\text{TCNQH}^-$ , i.e.,  $pK_{a5} > pK_{a4}$ , which is the usual situation for quinone species. The intersection of the two straight lines in Figure 7 gives  $pK_{a5} = 6.9$  for the  $\text{TCNQH}_2$  units in the polymer matrix. Extrapolation of the  $E_{1/2}$  data of Figure 7 to  $E_{1/2}^{-/2-} \approx -0.35 \text{ V}$  vs. SCE allows us to estimate  $pK_{a6} \approx 10$  for dissociation of the

**Scheme II**



$\text{TCNQH}^-$  sites in the polymer matrix. It should be mentioned that this assignment of wave X to the  $\text{TCNQ}^{0-}/\text{TCNQH}^-$  couple implies no mechanistic knowledge of the order of electron or proton transfer for this process.

Comparison of these  $pK_a$  values with literature values of model compounds is of interest since apparently the  $pK_a$  of the unsubstituted  $\text{TCNQH}_2$ , *p*-phenylenedimalononitrile,<sup>39</sup> has not been reported. Although the influence of the polymer film matrix is difficult to assess, the above values seem reasonable since phenylmalononitrile has a  $pK_a$  of 5.80.<sup>40</sup> Substitution on the phenyl ring by two oxyethanol groups decreases the  $E_{1/2}$  of TCNQ by approximately 60 mV<sup>31</sup> and would be expected to increase the  $pK_a$  of  $\text{TCNQH}_2$  in a similar fashion; i.e.,  $\Delta E(F/2.3RT) \approx 1 \text{ pK}$  unit. Reduction of dilute solutions of unsubstituted TCNQ at a Hg-pool cathode in  $\text{HClO}_4/\text{ethanol}/\text{water}$  mixtures (pH  $\approx 1.5$ ) results in the disappearance of the 395-nm band of TCNQ and the appearance of very weak new bands at ca. 270 and 300–310 nm assigned to  $\text{TCNQH}_2$ , in agreement with the work of Yamagishi and Sakamoto.<sup>36</sup> Owing to the apparent oxygen sensitivity of the malononitrile anion<sup>41</sup> these solutions have proved to be difficult to study at high pH.

**pH Effects on the ESR Spectra.** In our previous study<sup>31</sup> the potential dependence of the ESR signal generated in TCNQ polymer-coated Pt flag electrodes was most informative. Maxima in these curves were interpreted as arising from a potential-dependent contribution from a mixed-valence species generated in the polymer film. Accordingly, the polymer film SEESR experiment was carried out in several acidic buffer solutions. The pH dependence of the single-line ESR signal in 0.5 M phosphate buffer is shown in Figure 8. At pH 7 the same general features are observed as were seen in the previous studies in 0.5 M alkali metal cation electrolytes. Maxima are observed on both the negative- and positive-going potential sweeps, and there is a marked hysteresis. No significant variation in the ESR signal is seen in the potential region of wave X. It should be noted, however, that a large decrease in the ESR signal would not be

(39) Acker, D. S.; Hertler, W. R. *J. Am. Chem. Soc.* **1962**, *84*, 3370.

(40) Briegleb, G.; Breber, A. *Z. Elektrochem.* **1951**, *55*, 150.

(41) Suchanski, M. R.; Van Duyne, R. P. *J. Am. Chem. Soc.* **1976**, *98*, 250.

(38) Laviron, E. *J. Electroanal. Chem. Interfacial Electrochem.* **1983**, *146*, 15.

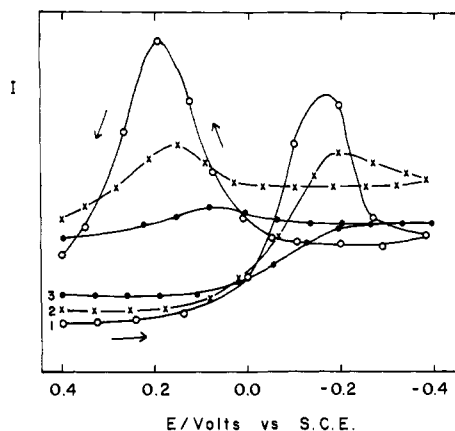


**Figure 8.** Potential dependence of the ESR signal intensity of a TCNQ film electrode in contact with (1) pH 7, (2) 5.3, and (3) 3.5, 0.5 mol dm<sup>-3</sup> phosphate buffer solutions.

expected since the TCNQ<sup>-</sup> absorbance is significant in this potential region (cf. Figure 2). Owing to the nature of the intramuros electrochemical generation technique used in these studies, the thin-film spectroelectrochemical experiments were performed under better defined conditions (current density, film uniformity, lack of edge effects, etc) than the SEESR experiments. Thus it is likely that changes in the ESR signal corresponding to the absorbance changes in Figure 2 would not be seen.

As the pH is decreased, and the maxima become less pronounced. The significant feature of these results is that the signal persists for long times at potentials positive of the TCNQ<sup>0/-</sup>  $E_{1/2}$  value for pH 3.5, 5.3, and 7 solutions. Evidently, the electrochemical cycling process has trapped radical sites in the TCNQ polymer film. This is the case even at pH 3.5 where absorption spectra of the reduced films do not show significant absorption bands for the radical anion species. It seems likely that a sizable fraction of the acceptor sites in the film possesses unpaired electron density, probably in the mixed-valent state which does not absorb in the visible or near-infrared spectral regions.<sup>28</sup> These trapped radical anion or dimer radical anion sites are viewed as being insulated in the bulk of the film by neutral TCNQ or TCNQH<sub>2</sub> layers that do not support a rapid charge-transport process.

**Chronocoulometry.** The decreased peak height and diffusional character of the TCNQ<sup>-</sup>/TCNQH<sup>-</sup> wave relative to the TCNQ<sup>0/-</sup> wave suggest that the apparent diffusion coefficient for charge transport through the film ( $D_{ct}$ ) has decreased. As shown by Buttry and Anson<sup>18</sup> in several papers, markedly different  $D_{ct}$  values can be seen for successive electron-transfer steps in a given polymer matrix when the Dahms-Ruff electron-exchange diffusion mechanism is operative. In these TCNQ polymer films for the first wave exchange occurs between TCNQ and TCNQ<sup>-</sup> sites, while for wave X, exchange is between TCNQ<sup>-</sup> and TCNQH<sup>-</sup> sites. The latter will probably involve a proton-transfer step (rather than hydrogen-atom transfer) and consequently should be pH dependent. For example, the following sequence is likely: TCNQ<sup>-</sup> + TCNQH<sup>-</sup> ⇌ TCNQ<sup>2-</sup> + TCNQH<sup>·</sup> ⇌ TCNQH<sup>-</sup> + TCNQ<sup>-</sup>. Since Laviron<sup>38</sup> has predicted the decrease of the effective rate constants for electron-transfer reactions in surface electrochemical reactions with equilibrium protonations, it was of interest to determine the  $D_{ct}$  values for the TCNQ<sup>-</sup>/TCNQH<sup>-</sup> process.

Chronocoulometric experiments were performed on TCNQ film electrodes in a pH 7, 0.5 M phosphate buffer where the TCNQ<sup>-</sup>/TCNQH<sup>-</sup> wave is well developed. Successive potential steps from +0.300 to -0.135 V and then from -0.135 to -0.300 V were applied to a series of electrodes. The total charge ( $Q_T$ ) injected into the film was typically much larger for the first than for the second potential step. Furthermore, a plateau value of

$Q_T$  was usually reached within a few seconds for the TCNQ<sup>0/-</sup> wave as would be expected for full film electroactivity. Using the total concentration of exchange sites from previous measurements,  $C_T = 3.6$  mol dm<sup>-3</sup>,<sup>31</sup>  $D_{ct}$  values of  $5 \times 10^{-11}$  and  $6 \times 10^{-13}$  cm<sup>2</sup>/s were derived from the data with use of the integrated form of the Cottrell equation. The 100-fold difference can be related either to the coupled protonation equilibria or slow electron transfer. The TCNQH<sup>-</sup> (and TCNQH<sub>2</sub>) structures are nonplanar and thus slower electron transfer is to be expected between TCNQ<sup>-</sup> and TCNQH<sup>-</sup> than between the planar TCNQ, TCNQ<sup>-</sup>, and TCNQ<sup>2-</sup> structures.

## Conclusions

This study has demonstrated that polymer film electrochemistry can be markedly dependent on the presence of buffer components in the supporting electrolyte to an extent beyond the usual role of pH for solution redox couples. For these TCNQ polymer films at low pH, electrochemical reduction results in film passivation due to formation of an insulating TCNQH<sub>2</sub> layer that does not support charge transport. Full electroactivity is restored when the film is returned to neutral electrolyte solutions.

At intermediate pH ranges, in the presence of buffer components which can protonate the TCNQ<sup>2-</sup> dianion sites in the polymer matrix, the second electron transfer, the TCNQ<sup>-</sup>/TCNQH<sup>-</sup> wave, becomes markedly attenuated relative to the TCNQ<sup>0/-</sup> or the TCNQ<sup>-/2-</sup> waves. Effective diffusion coefficients for charge transport are decreased by 100-fold due to the coupled proton-transfer steps. At higher pH (>8) the film electrochemistry is not complicated by the protonation reactions. These results can be understood with the aid of Scheme II with  $pK_{a5} = 6.9$  and  $pK_{a6} = 10$  for the TCNQH<sub>2</sub> sites in the fully protonated reduced film. Thus the classical square scheme depicting the coupling of electron- and proton-transfer steps for quinone systems<sup>32,42</sup> describes the electrochemical behavior of these TCNQ polyester films. The following thermodynamic parameters can be derived for the fixed TCNQ electron-transfer sites:  $E^\circ(\text{TCNQ}/\text{TCNQ}^-) = +0.02$  V vs. SCE,  $E^\circ(\text{TCNQ}^-/\text{TCNQ}^{2-}) = -0.35$  V vs. SCE,  $pK_a(\text{TCNQH}_2/\text{TCNQH}^-) = 6.9 \pm 0.1$ , and  $pK_a(\text{TCNQH}^-/\text{TCNQ}^{2-}) = 10$ , in 0.5 mol dm<sup>-3</sup> sodium ion electrolytes.

The high concentration (>1 mol dm<sup>-3</sup>) and basic character of the TCNQ<sup>-</sup> and TCNQ<sup>2-</sup> sites imply that the hydroxide ion concentration and the pH will be appreciable in the reduced films. This explains the absence of the TCNQ<sup>-</sup>/TCNQH<sup>-</sup> wave and suggests an explanation for the film instability and dissolution in the -2 oxidation state in unbuffered, neutral electrolytes. Hydrolysis of the adipoyl ester links will take place at high pH, and the film will dissolve. This is the observed behavior when the films are cycled to potentials more negative than the TCNQ<sup>-/2-</sup> wave.<sup>28</sup> In CaX<sub>2</sub> electrolytes, however, apparently the hydroxide ion is complexed with the calcium ion and the film is stable in this potential range.

These results emphasize the role of coupled chemical reactions in the polymer film charge-transport process and the design of polymer-modified electrodes. Most applications envisioned for these devices require facile charge transport through the film. But as shown in this study the coupling of proton- and electron-transfer reactions in a polymer film phase can significantly decrease the charge-transport rate and limit film electroactivity to a fraction of the available electron-transfer sites.

**Acknowledgment.** This research was supported by the U.S. Army Research Office (Project No. P-17715-C).

**Registry No.** Pt, 7440-06-4; NaClO<sub>4</sub>, 7601-89-0; (2,5-bis(2-hydroxyethyl)TCNQ)-(adipoyl chloride) (copolymer), 83462-96-8; poly(adipoyl 2,5-bis(2-hydroxyethyl)TCNQ), 83462-97-9.